

FIELD MEASUREMENTS IN A PINCH DISCHARGE USING A MAGNETO-OPTICAL PROBE

by

P Smeulders

(To be submitted for publication in J.Phys.D,Appl.Phys.)

ABSTRACT

This paper describes a miniature shaped glass magneto-optical probe. The performance of it is measured and compared in a fast linear combined θ/z pinch device with that of a conventional induction probe. Because of the very good time response of the magneto-optical probe fast changes in the axial current distribution are seen. This information is new and was not obtained with the induction probe. Typically a field of 20 gauss and a band width of 50 Mc./s has been detected in the experiments described here. A design for a magneto-optical triple probe based on the performance of the single probe is described.

UKAEA Research Group
Culham Laboratory
Abingdon
Berkshire

February 1974

1. INTRODUCTION

The Faraday rotation in high density flint glass is fairly commonly used for measurements of magnetic fields. An important advantage over the conventional induction coil is the frequency independence up to 10 Gc/s⁽¹⁾. An application of a Faraday rotation or magneto-optical probe on a fast θ -pinch device has already been reported⁽¹⁾.

In order to measure the magnetic field components of a fast combined θ/z -pinch a specially shaped high density flint glass miniature probe (diameter $\phi=4\text{mm}$) has been designed⁽²⁾ and now successfully tested as described here.

With a magneto-optical triple probe, whose features will be outlined later, the three magnetic field components can be measured simultaneously.

2. THE MAGNETO-OPTICAL PROBE

The probe is made of SF57 high density flint glass. For the fields expected in the combined pinch experiment the Faraday ellipticity, the Voigt effect, the Kerr electro-optical effect and the magneto-reflection all give negligible ($< 10^{-7}$) birefringence compared with the Faraday rotation. This is readily seen from the formula given by Smith⁽³⁾ and Jenkins⁽⁴⁾. It follows that each magnetic field component can be measured independently and also unperturbed by electrical fields.

The angle of rotation of the light due to the Faraday effect is given by $\phi = V(\omega) B \ell \cos \alpha$; α is the angle between the light vector \underline{k} and the magnetic field vector \underline{B} ; ℓ is the light path, $V(\omega)$ is the Verdet constant and is a function of the angular frequency ω of the light: $V(\omega) = \frac{e}{2mc^2} \gamma \omega \frac{dn}{d\omega}$ where e , m and c have their usual meaning and γ is the ratio of the actual value and the classical-theoretical value, for SF57 γ is between 0.75 and 0.8 in the visible. The factor γ is well explained by Serber⁽⁵⁾ quantum-mechanically; n is the refractive index and is related to ω as follows:

$$n^2 = 1 + \frac{\omega_p^2}{\omega_0^2 - \omega^2} .$$

The constants ω_p and ω_o are calculated from data obtained from the manufacturer (Schott) and are respectively for SF57 1.73 and $1.16 \times 10^{16} \text{ sec}^{-1}$.

So in contrast to measurements which use the Faraday rotation in the plasma itself, one should use a light source of short wavelength, when using Faraday rotation in glass. Its relation to the signal from the light detector is given in detail in the appendix.

3. THE FAST COMBINED Z/θ PINCH

The 2 meter-linear programme pinch device⁽⁶⁾ has a fast axial magnetic field B_z of 20 kgauss rising in 7.5 μsec . The axial current was chosen to be 30 kA and also rises in 7.5 μsec . A slow B_z bias field of 300 gauss rising in 200 μsec and a preionisation axial current pulse of 15 kA are also applied. Figure 1 gives waveforms of the axial magnetic field (lower trace) and the axial current (upper trace). The quartz discharge vessel has a bore of 8 cm. A z-shell with a bore of 10 cm surrounds it. The gas filling pressure is 30 m Torr of hydrogen. The plasma temperature is between 30-60 eV as determined using diamagnetic loops and from the magnetic field profiles⁽⁷⁾, and the known density profiles⁽⁶⁾. On axis the value of β is ~ 0.3 and the density is about 10^{16} cm^{-3} ⁽⁶⁾.

4. THE OPTICAL APPARATUS

The probe is a cylindrical 90° roof top prism with a diameter of 4 mm and a total height of 6 mm. The angles of the probe are made within tolerances of 2 minutes of arc. The experimental optical arrangement is as sketched in Figure 2. The light source is a low power He - Ne laser, λ 6238 Å. The Calcite Rochon prism first polarises the light coming from the laser and then analyses the light which returns from the probe. The rotated component of the returning light is refracted at an angle of 10° by the Rochon prism. After passing through an interference filter this light is detected with a photomultiplier (RCA 7265).

The probe is held in a quartz envelope of an external diameter of 6 mm, which can be moved radially at midplane position in the discharge tube.

5. COMPARISON OF THE RESULTS OF THE MAGNETO-OPTICAL PROBE

AND THE INDUCTION PROBE

The induction probe consists of an array of four square double coil systems with a typical dimension of 3 mm. The bandwidth of the B_z coils is less than 10 Mc/s and of the B_θ coils is less than 5 Mc/s. The array is held in a quartz envelope with an outer diameter of 5 mm. The measurements⁽⁷⁾ at an axial current strength of 38 kA are compared with those with the optical probe.

The calibration of the inductive probe and of the optical probe in the case of the B_z field measurements is provided by discharges fired in vacuum. The absolute value of the B_z field is determined from the integrated signal of the flux loop. Corrections for the field perturbation due to the porthole in the z-shell are applied. Experimentally the correction is found to be $B_{\text{true}} = B_{\text{measured}}(1 + \epsilon)$ with $\epsilon = \epsilon_0 \exp(r/r_0)$; r in cm; $\epsilon_0 = 0.002$ and $r_0 = 0.89$ cm. The diameter of the porthole is 2.5 cm.

For the B_z measurements the whole surface area of the cylindrical prism probe is illuminated. This is in order to facilitate the optical alignment. In order to reduce the amount of stray light it was necessary for the B_θ measurements to collimate the laser beam down to 1 mm diameter, making the alignment procedure more difficult. This introduced a 10% error in the pathlength of the light in the probe.

6. MEASUREMENTS OF THE RADIAL PROFILE OF THE B_z FIELD

Figure 4 shows the comparison between the radial profile of B_z obtained with the inductive magnetic probe and that obtained with the magneto-optical probe. Agreement within 5% is seen for the magnetic field value on axis. Because the variation of the measured magnetic field value from discharge to discharge is about 1.5%, it is considered that the 5% difference on axis is due to a changed plasma diamagnetism, and not to the different nature of the probes, or to the fact that the diameter of the optical probe envelope (6 mm ϕ) was 1 mm bigger than the envelope of the induction coil (5 mm ϕ).

7. MEASUREMENT OF THE RADIAL PROFILE OF THE B_{θ} FIELD

Figure 5 shows the comparison between the radial profiles of the azimuthal magnetic field obtained with the inductive magnetic probe and with the optical magnetic probe in two series of measurements.

Agreement is within 15%. The error in the profile obtained with the induction probe is estimated from discharge to discharge variation and is $\sim 4\%$. The error in the magnetic field value obtained with the optical probe depends on the method chosen to calibrate the probe. The latter was calibrated in two ways. The first (marked in the figure by Δ) was obtained using the known value of B_{θ} at the wall from a Rogowski loop. The second way of calibrating the optical probe (marked by o) is with the aid of the preionization current distribution measured with the induction probe.

The errors in the first method are due to variations of the pathlength of the laser light in the probe at most 10%. The variations are caused by a slight changing optical alignment of the probe when it is placed at different radial positions.

The total error values up to $\sim 15\%$ due to an approximately 10% signal to noise level of the photomultiplier signal for the lower B_{θ} field values. The agreement of the B_{θ} values nearer to quartz wall is better $\sim 3\%$ mainly due to the radial position being closer to the calibrated position of the probe, so that less correction of the optical alignment is necessary.

The error in the second method is related to the 10% signal to noise level for the lower B_{θ} field measurements of the preionization current. This results in about 5% variations from the profile obtained with the induction probe. The bump in the profile 1 cm from axis is due to a collapsing cylindrical current sheath in the plasma which will be discussed in more detail.

8. THE TIME RESPONSE OF THE PROBES

One of the main advantages of the magneto-optical probe is its very large bandwidth. An example of its capabilities is the measured B_{θ} field given in figure 6 at three radial positions as a function of time. The output of the

photomultiplier is filtered by a 2×10^{-8} sec passive integrating system. The peaks due to passing narrow current sheaths, are clearly shown. To follow the very rapid change of the magnetic field poses no problem for the optical probe, which is not the case for the inductive probe used in these experiments due to its limited bandwidth (linear up to 3 Mc/s).

9. DISCUSSION

The existing probe proved to be capable of detecting magnetic fields from 20 gauss up to 20 kgauss, while using a He - Ne laser with a wavelength of 6328 Å and using SF 57 optical glass. By using a shorter wavelength and higher density flint glass, the Verdet constant (V) will increase by 1 or 2 orders of magnitude. Theoretically for SF 57 at 2000 Å; $V \sim 5 \text{ mingauss}^{-1} \text{ cm}^{-1}$. This would make it possible to detect with the same miniature probe as described here fields of ~ 0.5 gauss. Also the quantum efficiency of the photocathode of most photomultipliers increases with decreasing wavelength. The signal to noise ratio can also be improved by increasing the light intensity of the laser. This combined with a large bandwidth gives the following characteristics of an optical probe. Measurements are possible from the nanosecond region up to static magnetic fields and field strengths varying from a few gauss up to 100 kgauss (the latter according to Knoepfel⁽⁸⁾).

Further, with a "triple" magneto-optical probe as sketched in Fig 7, it will be possible to measure the three components of the magnetic field locally and instantaneously. The central part measures the B_r field and with the two sides one can measure the B_θ and B_z components. It should be pointed out that an absolute calibration of the magneto-optical probe can be obtained by rotating the probe about its axis as indicated in the appendix, or by inserting and rotating by known amounts a polariser in between the Rochon prism and the probe.

10. CONCLUSION

Good agreement is observed between the magnetic field radial profiles obtained with the magneto-optical probe and the inductive magnetic probe. The main advantage of the optical probe compared with induction probes is its very wide bandwidth up to 10 Gc/s. Further, no electrically conducting parts are inserted into the plasma, which is not the case when using other probe techniques. It is expected that the lower limit of measurement, 20 gauss at a bandwidth of 50 Mc/s, can be improved to 0.5 gauss for the same bandwidth. Because of its very good time response fast changes in the axial current distributions are seen with the optical probe, these changes were not quantitatively observable with the induction probe.

The proposed triple probe will make it possible to measure the three magnetic field components at the same time, at the same position in space and over a very wide frequency range with a greater accuracy than electrical methods for such conditions permit.

ACKNOWLEDGEMENTS

The author wishes to acknowledge the fruitful discussions he had with Dr I K Pasco and Dr D C Robinson, he also wishes to thank Dr H A B Bodin for his very useful comments on the paper.

APPENDIX

The polarised laser light traverses the probe as given in Figure 3. The light enters at the right hand side of the probe and is rotated by an amount ϕ_{PQ} if a magnetic field component parallel to PQ is present. At Q it encounters a phase shift which differs for the light component in the \underline{K}_i , \underline{a}_1 plane and the component perpendicular to it, according to the formula given in Weizel⁽⁹⁾. Because of this we split the electric vector of the incoming polarised light into two components written as follows:

$$\underline{E}_i = E_0 (\sin \alpha \underline{e}_\perp + \cos \alpha \underline{e}_\parallel) \cdot \cos(\underline{k}_i \cdot \underline{x} - \omega t)$$

and as indicated in Figure 3, $\underline{e}_\perp, \underline{e}_\parallel$ are unit vectors. The phase shifts are then for the \underline{e}_\perp components $\delta_{\perp 1}$ and $\delta_{\perp 2}$ for the shifts at Q and R respectively. Similarly for the \underline{e}_\parallel components $\delta_{\parallel 1}$ and $\delta_{\parallel 2}$.

Between Q and R the light components are rotated by the magnetic field components parallel with QR by an amount ϕ_{QR} . After the phase shifts at R the light components are, again if the magnetic field component parallel to RS or PQ is present, rotated by ϕ_{RS} . This all gives rise to a light component \underline{E}_p perpendicular polarised to the incoming light \underline{E}_i . After taking into account the stray light of same frequency we get for small rotations, the following formula for \underline{E}_p

$$E_p = E_0 \left[C \cos (\underline{k} \cdot \underline{x} - \omega t + \delta) + S \sin (\underline{k} \cdot \underline{x} - \omega t + \delta) \right]$$

$$\text{with } C = \sin 2\alpha \cos \mu - \cos 2\alpha (\phi_{QR} \cos \nu + (\phi_{PQ} - \phi_{RS}) \cos \mu) \\ + \int_{-\pi}^{\pi} \epsilon(\psi) \cos \psi \, d\psi$$

$$S = (\phi_{PQ} + \phi_{RS}) \sin \mu + \phi_{QR} \sin \nu + \int_{-\pi}^{\pi} \epsilon(\psi) \sin \psi \, d\psi$$

The terms containing $\epsilon(\psi)$ originate from the stray light which has an electric vector, that can be written in a general form as:

$$E_0 \int_{-\pi}^{\pi} \epsilon(\psi) \cos (\underline{k} \cdot \underline{x} - \omega t + \delta + \psi) \, d\psi .$$

Further

$$\mu = 0.5 (\delta_{\perp 1} - \delta_{\parallel 1} + \delta_{\perp 2} - \delta_{\parallel 2}) ; \nu = 0.5 (\delta_{\parallel 1} - \delta_{\perp 1} - \delta_{\perp 2} + \delta_{\parallel 2}) \text{ and}$$

$$\delta = 0.5 (\delta_{\perp 1} + \delta_{\parallel 1} + \delta_{\perp 2} + \delta_{\parallel 2}).$$

For the optical probe discribed here we find

$$\mu = 0 , \nu = 64.8^{\circ} ; \delta = 194.4^{\circ} \text{ and } \phi_{PQ} = \phi_{RS}.$$

The output of the photomultiplier is then derived from the formula for E_p as follows:

$$V_{PM} = V_o (C^2 + S^2) + V_r ; C \text{ and } S \text{ are as above and } V_r \text{ is the photomultiplier signal without the laser light; } V_o \text{ is proportional to } E_o^2 .$$

An absolute calibration of the probe is obtainable by measuring V_{PM} as a function of the angle α , if the Verdet constant of the probe is known.

REFERENCES

1. McCARTAN, J., BARRAULT, M.R., J. Sci. Inst. 44, pp.265 (1967).
2. SMEULDERS, P. 10th International Conference on Phenomena in Ionized Gases, Oxford, 1, pp.438, (1971).
3. SMITH, S.D., Handbuch der Physik, 25/2a, pp.234-318. Published Springer-Verlag, (1967).
4. JENKINS, F.A. and WHITE, H.E. Fundamentals of Optics, McGraw-Hill Book Company, New York (1957).
5. SERBER, R. Physical Review, 41, pp.489-506 (1932).
6. PASCO, I.K. Ph.D. Thesis, Polytechnic of North London (1972).
7. PASCO, I.K., ROBINSON, D.C. and SMEULDERS, P. Second Topical Conference on Pulsed High-Beta Plasmas, Garching, paper A6, p.37, (1972).
8. KNOEPFEL, H. Pulsed High Magnetic Fields, North Holland Amsterdam (1970).
9. WEIZEL, W. Lehrbuch der Theoretischen Physik I. Published by Springer-Verlag, (1963).

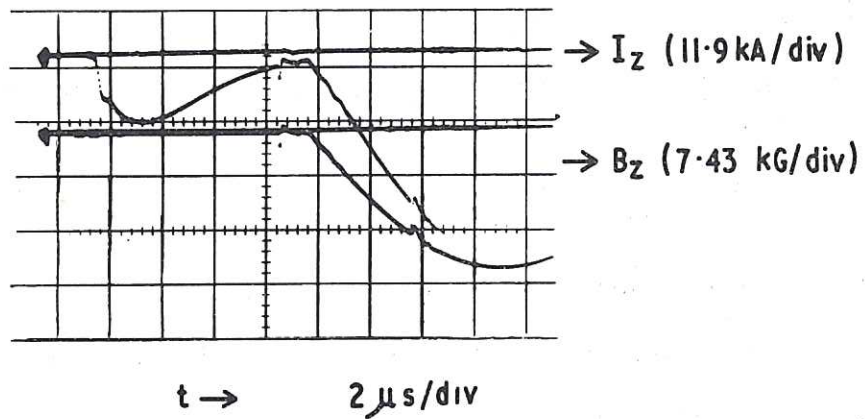


Fig.1 Upper trace: total axial current I_z (11.9 kA/div)
 Lower trace: the external axial magnetic field B_z (7.43 kG/div)
 both as a function of time (2 $\mu\text{sec/div}$).

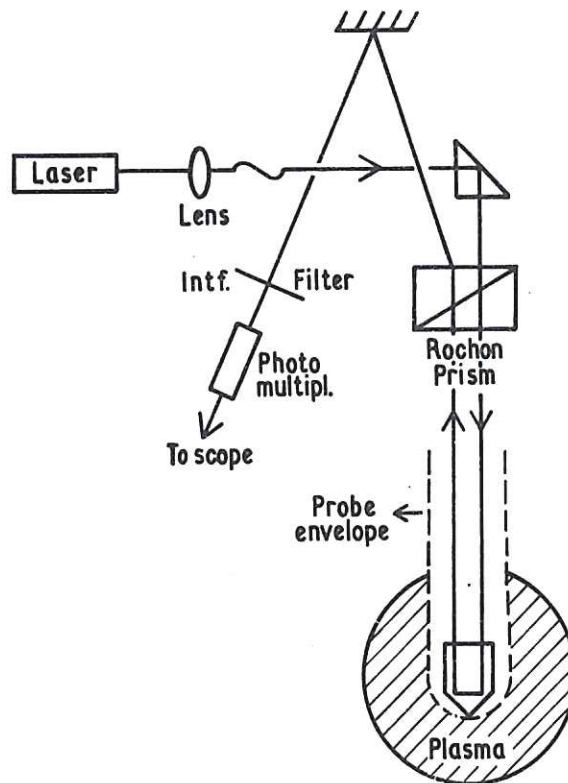


Fig.2 Optical arrangement of the magneto-optical probe.

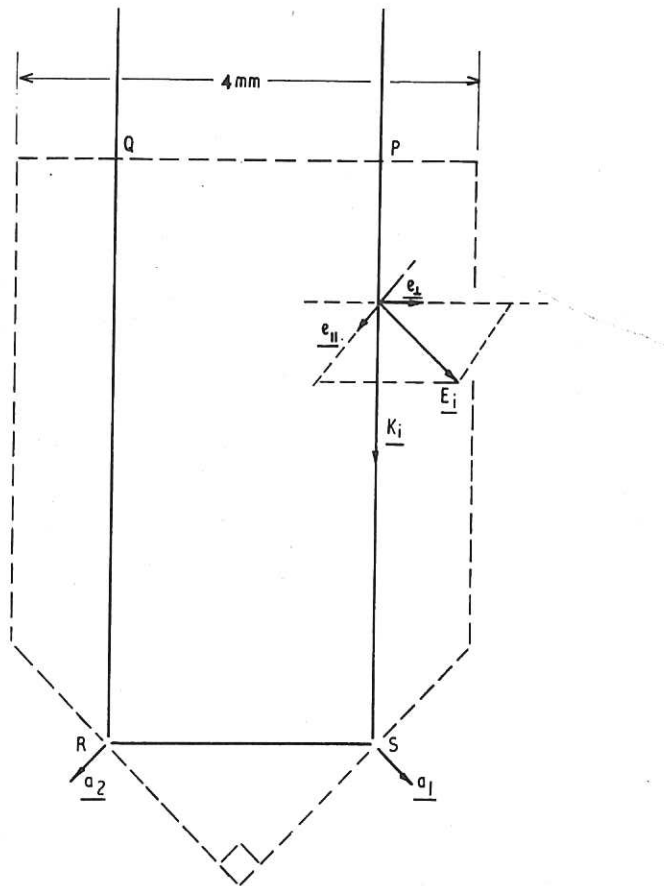


Fig.3 A cross-section of the magneto-optical probe; the light is indicated with a solid line.

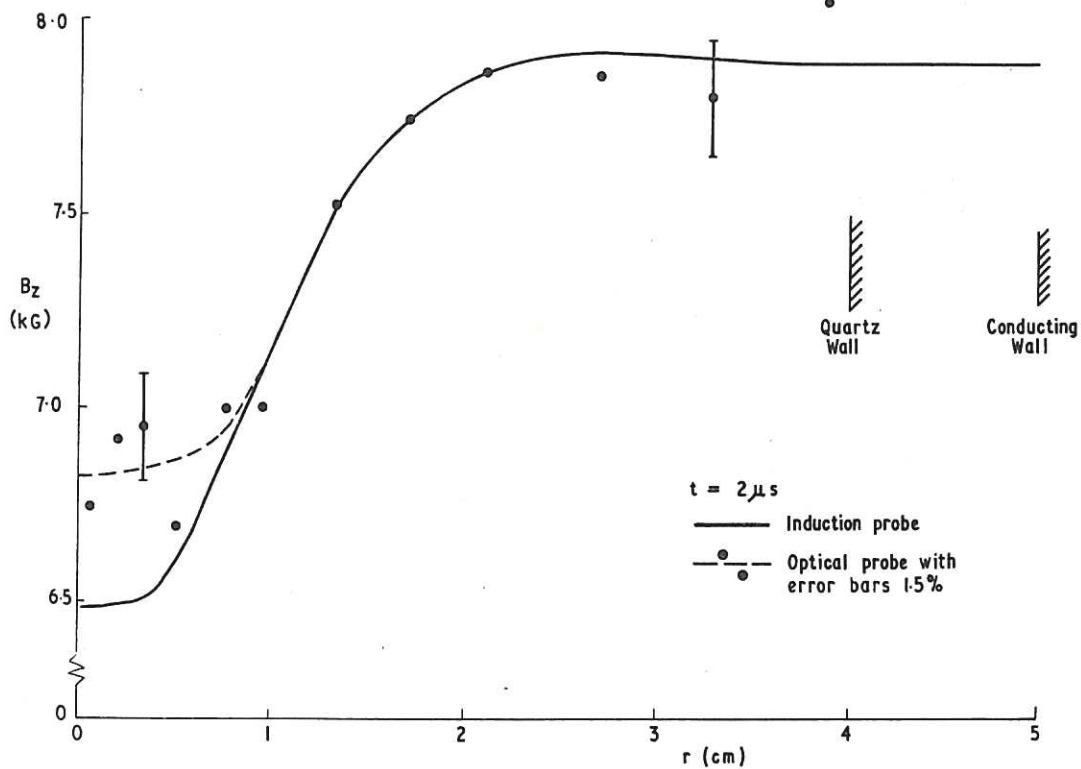


Fig.4 The radial profile of the axial magnetic field B_z at $t = 2 \mu\text{sec}$ from the start of the discharge measured by induction and magneto-optical probes.

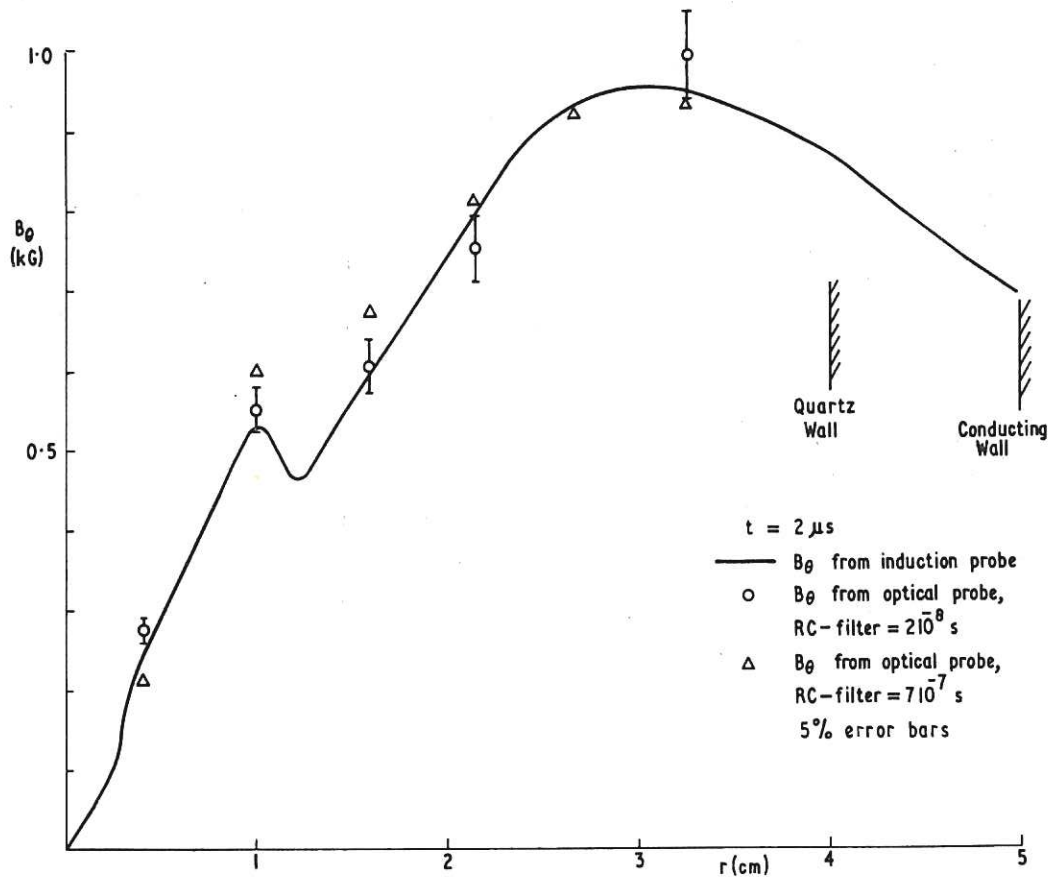


Fig.5 The radial profile of the azimuthal magnetic field B_{θ} at $t = 2 \mu\text{sec}$ from the optical and induction probes.

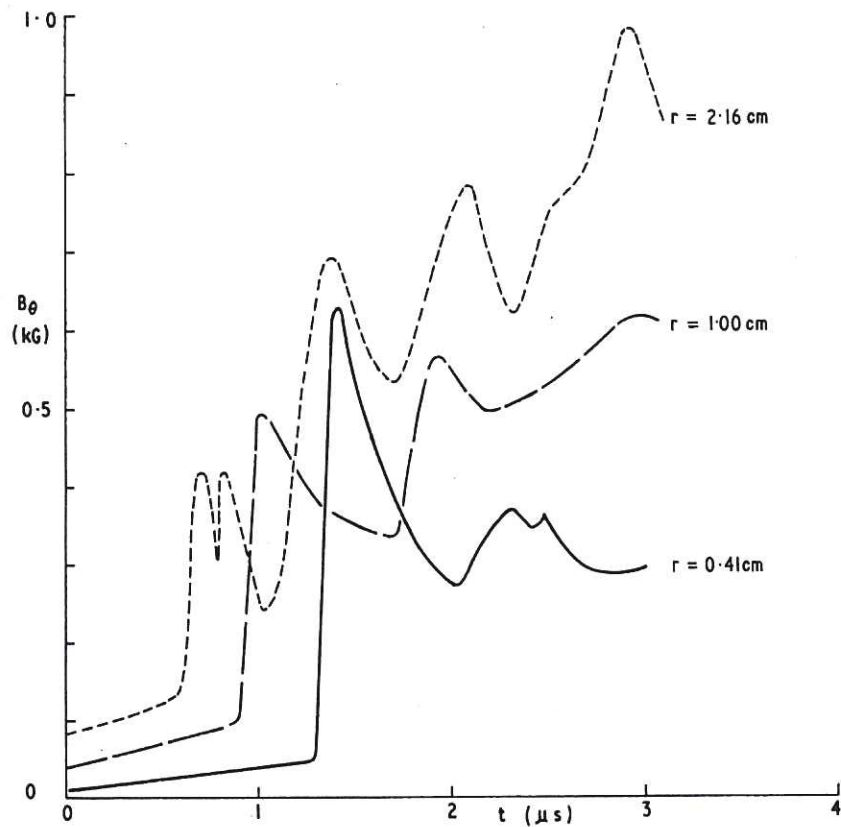
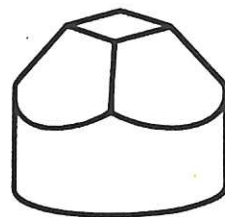
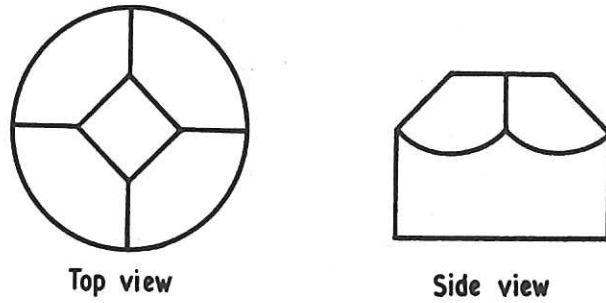


Fig.6 Time history of B_{θ} at different radial positions as measured with the magneto-optical probe.



Scale 10:1

Fig.7 Schematic view of the triple magneto-optical probe.

